Discovery of Pyrazolopyridones as a Novel Class of Noncovalent DprE1 Inhibitor with Potent Anti-Mycobacterial Activity

ARTICLE *in* JOURNAL OF MEDICINAL CHEMISTRY · MAY 2014

Impact Factor: 5.45 · DOI: 10.1021/jm5002937 · Source: PubMed

Journal of Medicinal Chemistry

Article

pubs.acs.org/jmc

Discovery of Pyrazolopyridones as a Novel Class of Noncovalent DprE1 Inhibitor with Potent Anti-Mycobacterial Activity

Manoranjan Panda,*[,†] Sreekanth Ramachandran,[†] Vasanthi Ramachandran,[‡] Pravin S. Shirude,[†] Vaishali Humnabadkar,[‡] Kavitha Nagalapur,[†] Sreevalli Sharma,[‡] Parvinder Kaur,[‡] Supreeth Guptha,[‡] Ashwini Narayan,[‡] Jyothi Mahadevaswamy,[‡] Anisha Ambady,[‡] Naina Hegde,[‡] Suresh S. Rudrapatna,[†] Vinayak P. Hosagrahara,[‡] Vasan K. Sambandamurthy,[‡] and Anandkumar Raichurkar[†]

[†]Department of Chemistry, [‡]Department of Bioscience, IMED Infection, AstraZeneca India Pvt. Ltd., Bellary Road, Hebbal, Bangalore 560024, India

Supporting Information

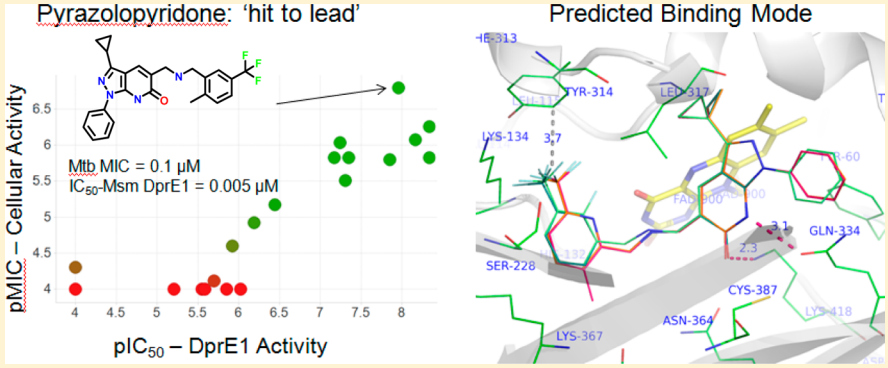

ABSTRACT: A novel pyrazolopyridone class of inhibitors was identified from whole cell screening against *Mycobacterium tuberculosis* (Mtb). The series exhibits excellent bactericidality in vitro, resulting in a 4 log reduction in colony forming units following compound exposure. The significant modulation of minimum inhibitory concentration (MIC) against a Mtb strain overexpressing the *Rv3790* gene suggested the target of pyrazolopyridones to be decaprenylphosphoryl-β-D-ribose-2′-epimerase (DprE1). Genetic mapping of resistance mutation coupled with potent enzyme inhibition activity confirmed the molecular target. Detailed biochemical characterization revealed the series to be a noncovalent inhibitor of DprE1. Docking studies at the active site suggest that the series can be further diversified to improve the physicochemical properties without compromising the antimycobacterial activity. The pyrazolopyridone class of inhibitors offers an attractive non-nitro lead series targeting the essential and vulnerable DprE1 enzyme for the discovery of novel antimycobacterial agents to treat both drug susceptible and drug resistant strains of Mtb.

INTRODUCTION

Tuberculosis (TB) continues to be a major cause of death each year, and the emergence of drug resistant strains of *Mycobacterium tuberculosis* (Mtb) has created a renewed demand to discover and develop novel drugs targeting this deadly pathogen.[1] Owing to the significant attrition in the lengthy course of discovery and development of new drugs, it is critical to continually develop new leads for tuberculosis in the discovery phase.[2]

Lead generation through whole cell screening (WCS) has proven to be a successful approach in drug discovery for infectious diseases.[3,4] While this approach circumvents the challenge associated with conversion of target potency (IC_{50}) to cellular potency (minimum inhibitory concentration, MIC), identifying the molecular target can be a rate limiting step, especially for a slow growing pathogen like Mtb. However, recent technological advances in genomics and proteomics have facilitated the identification of molecular targets for the hits originating from WCS as well as provide insights into the mode of inhibition.[5]

In one of our WCS-based lead generation approaches, we used a focused library from our corporate collection. The primary screen against Mtb H37Rv led to identification of multiple active series. The progression of various series through our screening cascade, including confirmation through compound resynthesis, assessment of cidality, and selectivity index, reduced the number of viable chemical classes. One of the most promising hits was the pyrazolopyridone class.

The "hit to lead" campaign for the pyrazolopyridones was driven by MIC-based structure–activity relationships (SAR). A parallel investment to identify the target led to the identification of decaprenylphosphoryl-β-D-ribofuranose-2′-epimerase (DprE1) encoded by the *Rv3790* gene as one of the potential

Received: February 24, 2014

   dx.doi.org/10.1021/jm5002937 | *J. Med. Chem.* XXXX, XXX, XXX–XXX

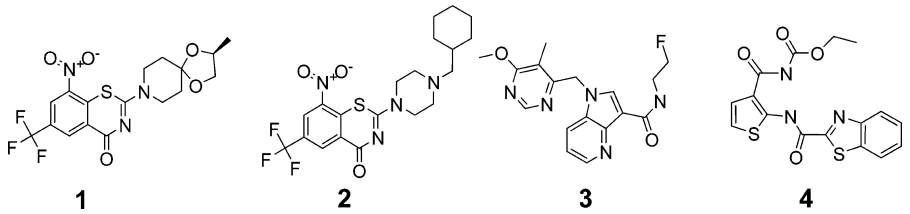

Figure 1. Literature reported inhibitors of Mtb DprE1. **1** and **2** bind covalently to the target, whereas **3** and **4** are noncovalent inhibitors.

targets for the series. DprE1, the key enzyme involved in the arabinogalactan biosynthesis, has been shown to be an essential target for the survival of mycobacteria.[6] Following the discovery of the nitrobenzothiazinone,[7] **1** (BTZ043) (Figure 1), that binds covalently to DprE1, there has been a growing interest in this target. The most recent preclinical candidate from the same class, **2** (PBTZ169),[8] has shown great promise as a new combination therapy for the treatment of tuberculosis. The recent report of the azaindoles (**3**, Figure 1), by Shirude et al.,[9] from one of our lead optimization programs and the benzothiazole,[10] **4** (TCA1, Figure 1), from Wang et al., have demonstrated that in vivo efficacy can be achieved via noncovalent inhibition of DprE1. Interestingly, all the DprE1 inhibitors reported to date emerged from a WCS approach.

RESULTS AND DISCUSSION

The initial hit (**5**) composed of a core *N*-aryl pyrazolopyridone ring with a basic amino linker attached to a phenyl ring gave a modest Mtb MIC of 25 μM. As shown in Table 1, we focused on the three diversification points at R_1, R_2, and R_3. Analogue testing from the corporate library revealed that phenyl rings at R_3 do not give any advantage compared to methyl substitution. On the basis of this observation, a methyl group at R_3 was fixed during initial MIC-based SAR exploration.

To understand the SAR for the substitution at the phenyl ring at R_1, we started with unsubstituted phenyl ring (**6**), which led to loss of activity. By varying the substitution patterns of the R_1 phenyl ring, we found *meta*-trifluoromethyl derivative **10** to show an 8-fold improvement in Mtb MIC as compared to **5**. Groups with similar size such as methyl (**7**) and electron withdrawing nature such as nitrile (**8**) at the *meta* position led to significant drop in activity. It indicated that the CF_3 group might be playing a critical role in binding to the active site. On the basis of the data from the limited exploration at R_2 (**11**–**13**), we fixed an unsubstituted phenyl ring as the preferred group. Small hydrophobic groups such as cyclopropyl at R_3 (**14**) resulted in the improvement of Mtb MIC. To reduce the lipophilicity and hence improve the physicochemical properties, the phenyl ring was replaced with the suitably substituted pyridyl ring (**15**). The comparison of data between the matched pairs **14** and **15** indicated that the drop in ClogP (~1.5 log) led to 4-fold decrease in potency. The improvement in Mtb MIC for the relatively higher log *P* compounds such as **14** for this series could be attributed to improved permeability across the Mtb cell membrane. Disubstitution on the R_1 aryl ring while retaining *meta*-trifluoromethyl (**16**–**21**) opened up new opportunities to improve the Mtb MIC. Comparison of the data from matched pairs (**10** vs **20**, **14** vs **19**, and **15** vs **18**) suggested that there is 4–10-fold improvement in Mtb MIC upon substitution of 6-methyl at R_1. In addition to enhancing the Mtb permeability, the methyl group at C-6 may be interacting favorably in the enzyme active site. The presence of 3-trifluoromethyl-6-methyl phenyl at R_1 (**19**) yielded an Mtb

Table 1. SAR of Functional Groups at R_1, R_2 and R_3 Led to Insight into the SAR and Hence Improvement in Mtb MIC

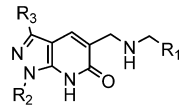

Compound	R_1	R_2	R_3	Mtb MIC (μM)	Mtb MBC (μM)	Msm DprE1 IC_{50} (μM)	ClogP
5		Ph	$-CH_3$	25	50	1.2	3.0
6		Ph	$-CH_3$	> 100	NA	1.4	2.0
7		Ph	$-CH_3$	100	100	2.8	2.5
8		Ph	$-CH_3$	> 100	NA	2.6	1.5
9		Ph	$-CH_3$	75	100	2.0	2.2
10		Ph	$-CH_3$	3.1	8.5	0.4	2.9
11			$-CH_3$	12.5	12.5	0.6	3.4
12			$-CH_3$	> 100	NA	NA	1.6
13		$-CH_3$	$-CH_3$	> 100	NA	> 100	1.0
14		Ph		1.6	2.8	0.04	3.4
15		Ph		6.3	5.6	0.05	2.0
16		Ph		1.6	4.4	0.07	3.5
17		Ph		1.6	4.1	< 0.005	3.5
18		Ph		1.5	1.6	0.01	2.5
19		Ph		0.1	< 0.5	0.01	3.8
20		Ph	$-CH_3$	0.8	1.2	0.007	3.4
21		Ph	-iPr	0.4	< 0.5	< 0.005	4.3

dx.doi.org/10.1021/jm5002937 | *J. Med. Chem.* XXXX, XXX, XXX–XXX

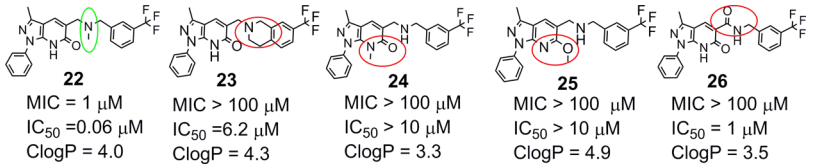

Figure 2. SAR exploration of linker and pyrazolopyridone ring.

Scheme 1. General Synthetic Scheme for Pyrazolopyridones

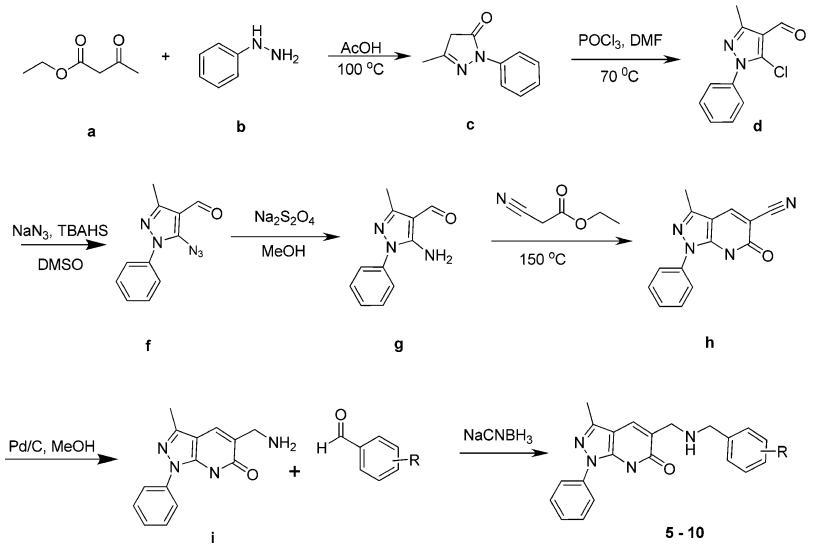

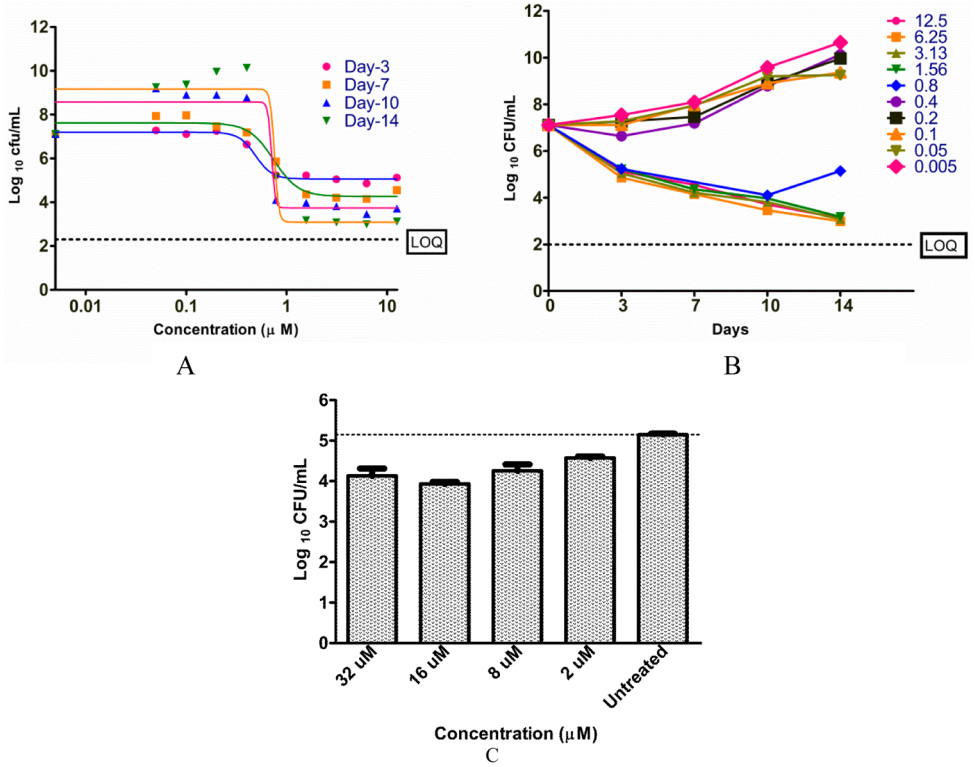

Figure 3. Killing kinetics (A,B) and intracellular efficacy (C) of compound **19** against Mtb.

MIC of 0.1 μM, the most potent compound in the series. Thus, our efforts to optimize the SARs have led to a remarkable improvement (>200-fold) in Mtb MIC from the starting point (**5**).

To understand the essentiality of the core pyrazolopyridone and the linker −NH, compounds **22**−**26** were synthesized (Figure 2). Compound **22** with the substituted *N*-methyl linker retained the Mtb MIC, whereas a cyclic tertiary amine such as **23** lost potency. Replacing pyridone with *N*-methylpyridone

dx.doi.org/10.1021/jm5002937 | J. Med. Chem. XXXX, XXX, XXX−XXX

Table 2. Pyrazolopyridones are Equipotent against Various Reference and Clinical Isolates of Mtb, Including Single-Drug-Resistant (SDR) Strains[a]

		MIC in μM						
Mtb strain names	source	**10**	**14**	STR	INH	RIF	ETM	OFL
H37Rv (ATCC27294)	sensitive[b]	3.1	1.6	0.3	0.2	0.02	2	0.7
Beijing (E-47/94)	sensitive[b]	3.1	1.6	0.3	0.2	0.02	2	0.7
D-211	sensitive[c]	3.1	1.6	0.3	0.2	0.02	2	0.7
STR^R (136570)	SDR[c]	3.1	1.6	>5	0.2	0.02	2	0.7
INH^R (912253)	SDR[c]	6.2	3.1	0.3	>29	0.02	2	0.7
RIF^R (19000)	SDR[c]	3.1	1.6	0.3	0.2	>5	2	0.7
ETM^R (17003)	SDR[c]	3.1	1.6	0.3	0.2	0.02	>20	0.7
OFL^R (12119)	SDR[c]	1.6	1.6	0.3	0.2	0.02	2	>5

[a]The MIC was determined following drug exposure, and growth was monitored by turbidometry. [b]Reference strains. [c]Clinical isolate: STR, streptomycin; INH, isoniazid; RIF, rifampin; EMB, ethambutol; OFL, ofloxacin.

Table 3. Pyrazolopyridones Lose Their MIC (μM) against Mtb Strain Over-Expressing DprE1 Gene and Recombinant Strains with Specific Mutations in the DprE1 Protein

compd	H37Rv WT	DprE1 OE strain	BTZ res mutant (C−G)	BTZ Res mutant (C−S)	**14**.Clone8.1	**14**.Clone8.2	**14**.Clone8.3
1	0.003	>0.1	>0.1	>0.1	0.002	0.003	0.002
10	5.0	>100	2.5	0.6	50	100	25
14	1.2	100	0.6	0.3	50	100	25
15	1.2	>100	0.3	0.3	100	>100	100
16	1.2	>100	0.3	0.1	>100	>100	50
17	1.2	100	0.6	0.3	100	100	100
19	0.1	>100	0.08	0.04	>100	>100	12.5
isoniazid	0.2	0.2	0.2	0.2	0.2	0.2	0.2

(**24**) or its isomeric form methoxypyridine (**25**) also resulted in the complete loss of potency, thereby suggesting that the pyridone moiety is essential. Similarly, replacing the −NH linker with an amide group (**26**) led to a loss of activity. The loss of Mtb MIC for compounds **23**−**26** despite having higher lipophilicity (log P > 3) clearly indicated that the series is specific, requires the key pharmacophores for its antitubercular activity, and is not correlated entirely with lipophilicity.

Synthesis of these pyrazolozopyridones proceeded through the previously reported[11] intermediate (**h**) starting from the condensation of commercially available ethyacetoacetate and phenyl hydrazine (Scheme 1). Hydrogenation of intermediate **h** under Pd/C condition followed by reductive amination with various aldehydes provided pyrazolopyridone derivatives **5**−**10**. Similarly, the compounds **11**−**21** were synthesized starting from the corresponding β-ketoester and hydrazines.

Microbiological Profile. Pyrazolopyridones were highly bactericidal against replicating Mtb with the ratio of Mtb MBC (minimum bactericidal concentration) and Mtb MIC close to one (Table 1). A detailed time course study using compound **19** as a representative showed a pronounced time-dependent killing over a period of 14 days with limited effect of compound concentration. By day 10, >4 log reduction in colony forming units (CFU) (Figure 3A,B) was observed. To further evaluate the potential of the pyrazolopyridones for activity against slowly replicating Mtb residing in macrophages, we exposed varying concentrations of **19** to THP-1 macrophages infected with Mtb. Following 7 days of exposure, **19** exhibited ∼1 $\log_{10}$ reduction in CFU at 16 μM (Figure 3C). These data demonstrate that pyrazolopyridones are active against slowly replicating Mtb residing inside macrophages, an important physiological milieu relevant in the pathogenesis of human tuberculosis.[1] The potential of the series against nonreplicating mycobacteria was assessed by determining Mtb MIC under hypoxic conditions. The results for a representative set of compounds (Supporting Information Table S1) suggest that the series does not possess any significant activity against nonreplicating Mtb.

To understand the antibacterial spectrum of the series, a few potent compounds were tested against a panel of bacterial strains comprising medically important Gram positive as well as Gram negative pathogens as described earlier.[9] These compounds lacked any appreciable antibacterial activity (MIC > 100 μM) against *Escherichia coli*, *Haemophilus influenzae*, *Staphylococcus aureus*, *Streptococcus pneumoniae*, *Pseudomonas aeruginosa*, *Klebsiella pneumoniae*, *Streptococcus pyogenes*, and *Candida albicans*, suggesting the target to be specific for mycobacteria.

MIC against Single Drug Resistant Strains of Mtb. To determine whether the pyrazolopyridone class has a novel mechanism of action, we tested compounds **10** and **14** against a panel of reference strains including several clinical single drug resistant strains of Mtb obtained from various sources. As shown in Table 2, **10** and **14** were equipotent against strains known to be resistant to the front line TB drugs such as isoniazid, rifampicin, ethambutol, streptomycin, and ofloxacin. This data reiterates the novel mechanism of action of pyrazolopyridones and their potential to be a part of a combination treatment for drug resistant TB.

Mode of Action Studies. To understand the mechanism of action, representative pyrazolopyridones were screened against the in-house available Mtb strains overexpressing several essential targets. The MIC modulation was observed only with Mtb strain overexpressing the *Rv3790* gene which encodes decaprenylphosphoryl-β-D-ribofuranose-2′-epimerase 1 (DprE1). As shown in Table 3, the compounds displayed a significant increase in their MIC in the overexpression strain, thereby suggesting the molecular target to be DprE1. DprE1 is a flavin adenine dinucleotide (FAD) dependent oxidoreductase

dx.doi.org/10.1021/jm5002937 | J. Med. Chem. XXXX, XXX, XXX−XXX

and is shown to be essential for the survival of mycobacteria.[6] The most advanced compounds targeting this enzyme are shown to be pro-drugs (**1** and **2**, Figure 1) that upon activation covalently bind to cys387 of DprE1.[8,12]

To provide a further genetic link to the mechanism of action, we isolated spontaneous resistant mutants to compound **14**. Mutants against compound **14** arose at a frequency of 6.7×10^{-8} when selected on agar plates containing 6.2 μM and at 3.8×10^{-9} when selected on agar plates containing 12.5 μM of compound. Six random resistant clones were characterized microbiologically for cross resistance to **14**, close analogues as well as standard TB drugs with different mechanisms of action to rule out nonspecific resistance. As shown in Table 3, compound **14**-resistant mutants showed an increase in MIC specific to **14** and its close analogues. However, the mutants displayed no cross resistance to other standard TB drugs. This data confirms the specificity of genetic mutations that confer resistance to pyrazolopyridones. To further characterize the genetic basis of resistance, we sequenced the entire *Rv3790* gene of four independent resistant clones. We found a single nucleotide change in the *Rv3790* gene resulting in an amino acid substitution at position 314 from tyrosine to histidine (Y314H, Figure 4). This mutation was previously reported to

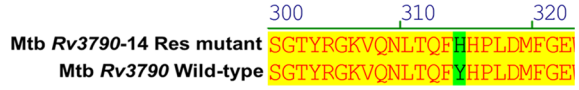

Figure 4. Mutation at Y314H observed from compound **14** resistant mutant.

confer resistance to azaindoles, another class of DprE1 inhibitors.[9] The mutation mapping data along with the MIC modulation observed in the overexpression strain strongly support the target of these novel pyrazolopyridones to be DprE1. Interestingly, pyrazolopyridones showed enhanced potency against the resistant strains of the compound **1** (Cys387Ser and Cys387Gly; Table 3) as compared to the wild-type strain.

Biochemical Screening against DprE1. To further establish the mode of action, we tested pyrazolopyridones for the inhibition of purified DprE1 from *M. smegmatis* (Msm) using a fluorescence-based assay.[9] DprE1 protein is highly conserved across mycobacteria,[7] with a sequence identity of amino acids between Mtb and Msm of 83%, and the active site is fully conserved.

The compounds were confirmed to be potent inhibitors of DprE1. The scatter plot of correlation between IC_{50} (Msm DprE1) and Mtb MIC is shown in Figure 5.

We observed a strong correlation between Msm DprE1 IC_{50} and Mtb MIC (Figure 5). The MIC-based SAR for the R_1, R_2, and R_3 groups (**5**–**21**) and pyrazolopyridone core (**22**–**26**) are in excellent agreement with the IC_{50}-based SAR obtained from Msm DprE1 enzyme assay (Table 1). The total enzyme concentration in the assay was 75 nM. Contrary to the expectation that the lowest measurable IC_{50} is half the enzyme concentration, compounds **17**–**21** exhibited IC_{50} < 37.5 nM. This can be attributed to the fact that only a fraction of total enzyme in the assay was catalytically active.

The activities of pyrazolopyridones against a mutant (Y321H) enzyme were also measured. The compounds were weaker inhibitors, with 40–150-fold shifts in IC_{50} with the mutant enzyme (Table 4). These data are in agreement with

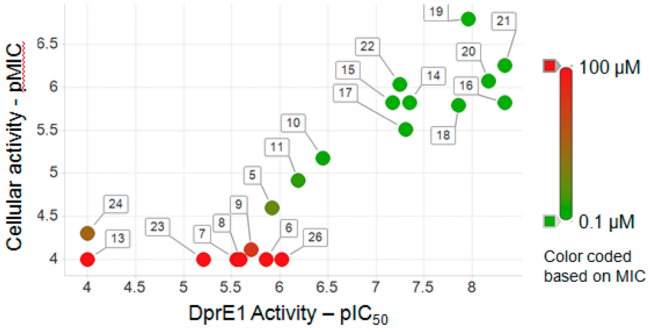

Figure 5. Scatter plot of enzymatic activity (Msm DprE1 IC_{50} in log scale) and cellular activity (Mtb MIC in log scale). The compound numbers are labeled.

Table 4. Shift in IC_{50} in the Mutant Enzyme

	Msm DprE1 IC_{50} in μM			fold shift in IC_{50}	
compd	WT[a]	C394G	Y321H	C394G/WT[a]	Y321H/WT[a]
15	0.15	0.02	6.1	−6	40
16	0.04	0.01	4.5	−4	107
17	0.22	0.06	8.2	−4	38
19	0.01	0.01	7.4	1	740
20	0.01	0.01	1.5	1	150

[a]WT = wild type. The fold shift in negative numbers indicate the modulation in reverse direction, in this case the compounds are more active in C394G mutant than the wild type.

the mutation mapping and the MIC modulation data seen for the series (Table 3). Additionally, these data implied the importance of tyrosine residue at position 314 for Mtb (Tyr321 in Msm), which is part of the active site. The compounds showed about 4–6-fold improvement in IC_{50} against the Cys394Gly mutant Msm enzyme resistant to **1**, in concordance with an improvement in MIC observed against an Mtb strain harboring the corresponding Cys387Gly mutation (Table 3). This indicated that Cys387, which forms covalent adduct with nitrobenzothiazinone class of inhibitors (**1** and **2**), is inconsequential to the binding of pyrazolopyridone, in turn the mutation to serine or glycine may be improving the free energy of binding. In addition, the Cys387Ser and Cys387Gly mutation may be affecting the permeability of the mycobacterium cell wall that is reflected in the improvement in Mtb MIC (Table 3). However, further investigation is required to probe this interesting observation.

Proposed Binding Mode of Pyrazolopyridone in the Active Site of DprE1. Several crystal structures of DprE1 bound to both covalent and noncovalent inhibitors have been reported. In the case of aromatic nitro compounds (nitrobenzothiazinones[13] and nitrobenzene[14]), the activated nitro group forms a covalent linkage with Cys387 (Cys392 is corresponding residue in Msm DprE1). Most recently, Wang et al.[10] published a co-crystal structure of one of the noncovalent inhibitors, **4** (Figure 1). The analyses of all these crystal structures showed no significant change in the conformation and shape of the active site and the cofactor, FAD. Except for the structure reported by Batt et al. with a noncovalently bound nitrobenzene, **27** (CT319),[14] (Table 6), all the reported structures showed two disordered loops close to the active site residues 269–283 and residues 314–322, thus making the active site partially open. The structure reported with **27** showed ordering of residues 314–322, which was attributed to

dx.doi.org/10.1021/jm5002937 | J. Med. Chem. XXXX, XXX, XXX–XXX

the mode of binding of the inhibitor. Sitemap[15] analyses of both the open and closed forms of the active site suggested that the site is highly druggable (Supporting Information). One of the striking features of the active site is the presence of highly functionalized residues such as Lys413, Ser228, Gln336, Gln334, Asn385, Tyr314, Trp230, Lys134, His132, and Trp60. The recent reports of a large number of DprE1 inhibitors with different pharmacophores could be attributed to this feature.

We performed docking using both open (pdb ID: 4KW5) and closed (pdb ID: 4FDO) forms of the active site. Glide 6.0 (Schrodinger)[16] was used without any constraints. The docking protocol reproduced the crystallographic poses of **4** and **27**. We obtained multiple possible modes of binding for pyrazolopyridones. The one that is consistent with the resistance mutation and biochemical activity is shown in Figure 6. The pyridone

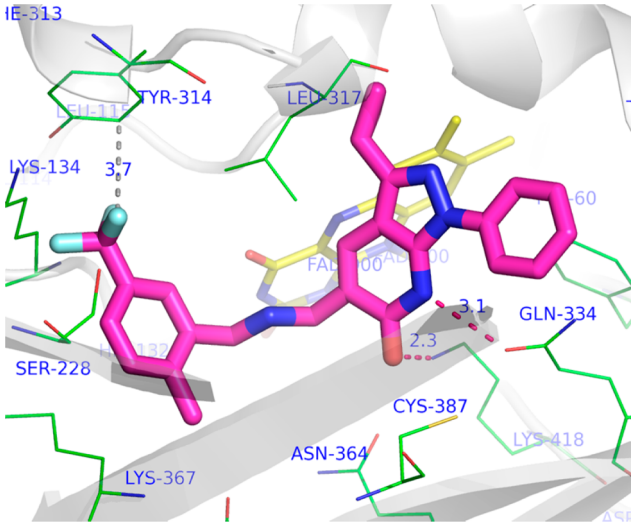

Figure 6. Glide docking pose of compound **19** in the DprE1 active site.

carbonyl oxygen atom and NH H-bond with Lys418 and Gln334, respectively. This is consistent with the SAR observation that alteration of this two donor/acceptor functionality led to inactive compounds (**24** and **25**, Figure 2). The CF_3 group occupies the hydrophobic pocket formed by the residues such as Leu317, Tyr314, and Lys134, thus explaining the importance of *m*-CF_3 on the R_1 aryl ring toward the activity (Table 1). The predicted pose showed multiple van der Waals contacts between phenolic side chain atoms of Tyr314 and the CF_3 group, the distance between two closest non-hydrogen atoms being 3.7 Å. The improvement in potency for compounds having a 2-methyl-5-trifloromethyl aryl group at R_1 (**18**−**21**) could be attributed to the hydrophobic contact between the 2-methyl group of the ligand and the methylene side chain of Lys367. Additionally, the 2-methyl group could be helping in optimal orientation of the CF_3 group. The −NH linker is within H-bonding distance of the carbonyl oxygen of the tricyclic ring of FAD in most of the docking poses. At physiological pH, this N atom is likely to be protonated, strengthening the polar interaction with the H-bond acceptors of the FAD ring. Replacing the amine with amide (**26**) not only changes the nature of the molecule from basic to neutral, it also affects the orientation of the trifluoromethyl substituted aryl ring at R_1 because of the planar nature of amide group, thus rendering this compound significantly weaker (Figure 2).

Key Challenges Associated with Pyrazolopyridone. We profiled the series for in vitro DMPK properties, preliminary toxicity such as cytotoxicity. The most potent compounds have log *D*s of 3.5 or higher and, consequently, solubility, free plasma protein binding, and clearance, are suboptimal (Table 5). Although the human microsomal clearance was acceptable, the rat liver hepatocytes clearance was found to be high. For monosubstitued aryl at R_1, a pyridyl ring in place of phenyl lowered the log *D* (matched pair: **14** vs **15**) by 0.7 unit, which is reflected in improved solubility. In the case of 2,5-disubstituted derivatives (matched pairs: **18** vs **19**), the pyridyl ring did not exhibit any significant improvement in physicochemical properties. However, the solubility of these disubstituted derivatives is improved as we go from cyclopropyl (**19**) to isopropyl (**21**) to methyl (**20**). These structure−property relationships (SPR) clearly indicate that these issues can be mitigated with suitable substitution in a lead optimization program.

Table 5. In Vitro DMPK and Safety Tests of a Few Selected Pyrazolopyridones

	14	15	18	19	20	21
Mtb MIC (μM)	1.5	3.1	1.5	0.1	0.8	0.4
aq solubility (μM)[a]	1	153	1	<1	55	10
measured log *D*	3.9	3.2	3.4	3.9	3.7	>4.4
Hu PPB (%) free	1	1.1	<1	<1	<1	<1
Hu microsomes[b]	27	19	26	29	67	32
rat hepatocytes[b]	320	368	375	361	519	303
selectivity index[c]	10	20	10	>250	20	35

[a]Kinetic solubility in the test media were >50 μM for all compounds. [b]Human microsomal Clint and Rat hepatocyte Clint are in μL/min/kg. [c]Selectivity index = IC_{50} against human A549 cell line (μM)/Mtb MIC (μM).

To understand the safety margin associated with the series, we tested the activity of a few compounds against the human A549 cell line (mammalian MIC). Even though the selectivity index was >10 for most compounds, the absolute mammalian MIC values were in the range of 30−100 μM. This could be largely attributable to the basic N atom and higher log *D* associated with the series. During the course of the medicinal chemistry optimization of the series, we focused on improving cytotoxicity. Appropriate substitution on the aryl ring at R_1 led to an improvement in cytotoxicity and thereby widening the selectivity index (SI). This effort resulted in SI index >250 for the most potent compound **19**.

The series was not profiled for its in vivo properties as the in vitro DMPK data such as solubility, plasma protein binding, and clearance for the series needs further optimization. Given the translation of in vitro biochemical and microbiological properties of recently reported noncovalent inhibitors of DprE1[9] into in vivo efficacy in a murine model of TB, pyrazolopyridones, with their excellent antimycobacterial properties, is highly likely to exhibit the in vivo efficacy upon optimization of DMPK properties.

Reported Noncovalent Inhibitors of DprE1 and Way Forward. The discovery of these novel pyrazolopyridones in conjunction with other reported DprE1 inhibitors, both covalent and noncovalent, has opened multiple avenues to

dx.doi.org/10.1021/jm5002937 | J. Med. Chem. XXXX, XXX, XXX−XXX

Table 6. Comparison of Molecular Properties of Covalent and Noncovalent Inhibitors of DprE1[a]

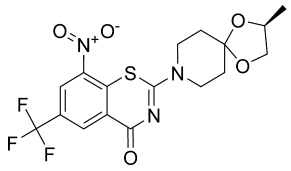

1

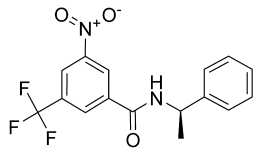

27

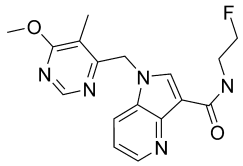

3

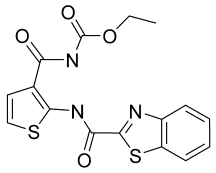

4

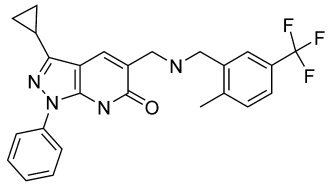

19

	1	27	3	4	19
MoI	covalent	covalent	noncovalent	noncovalent	noncovalent
MW	431	338	343	375	452
ClogP	2.4	4.3	1.5	3.6	3.8
MIC	0.004	0.94.3	1.51.5	0.5	0.1
IC_{50}	0.005	NA	0.005	NA	0.01
mutation	C387S	C387S	Y314H	Y314C	Y314H

[a]MoI = mode of inhibition; MW = molecular weight in Da; ClogP = calculated log *P*; MIC = cellular activity against Mtb in μM unit; IC_{50} = enzymatic activity against Msm DprE1 in μM unit; Mutation = resistant mutant mapping in Mtb DprE1.

target this essential mycobacterial enzyme with the aim of identifying a novel TB drug. These studies provide an attractive array of novel leads against DprE1 that span a wide range of physicochemical spaces (Table 6). The in vivo efficacy demonstrated for noncovalent inhibitors of DprE1 such as **3** and **4** have established that DprE1 can be targeted by noncovalent and non-nitro compounds. Additionally, the differential modes of inhibition and mutation (Cys387Ser vs Tyr314His) provide further impetus to invest in the development of both kinds of inhibitors.

From a medicinal chemistry perspective, it is exciting to see the emergence of different chemical classes targeting DprE1 with established SARs both for biochemical and antimycobacterial activity. Aside from DNA gyrase,[17] DprE1 is arguably the only current target that offers such a repertoire of lead generation opportunities against Mtb, with a strong correlation between enzyme inhibition and antimycobacterial activity. The reported crystal structures and SAR knowledge from different chemical classes sets the stage for structure-based lead optimization and lead hopping to find attractive candidate drugs acting against DprE1. The overlays of pyrazolopyridones with crystallographic poses (Figure 7) suggest that the series can be further optimized to mitigate the issues discussed above. The shape and pharmacophoric-based overlay[18] with an azaindole (Figure 7C) leads to several interesting medicinal chemistry designs such as disubstituted heteroaromatic rings at R_2 of pyrazolopyridone, alternate fused heteroaromatics rings in the place of core. These ideas may improve the in vitro DMPK properties without affecting the potency of the series.

CONCLUSION

In this work, we have established the pyrazolopyridones as a novel antimycobacterial lead series with attractive microbiological properties. The series exhibited >4 log reduction in CFU against replicating Mtb in broth. We established DprE1 as the target through mutant mapping and biochemical inhibition of the target enzyme. This is one of the first reports of a non-nitro and noncovalent inhibitor of DprE1. Using the reported crystal structures of DprE1, we proposed a mode of binding for the series consistent with the structure−activity relationship. During hit to lead exploration, we identified issues such as poor physicochemical properties and moderate activity against the human A549 cell line that could be largely attributed to high log *D* of the series. On the basis of the medicinal chemistry exploration, we have shown multiple diversification points to mitigate these issues. The knowledge from the reported crystal structures and the proposed model of binding could be further utilized to progress the lead series. Our finding of pyrazolopyridone series as a novel inhibitor of DprE1 in conjunction with recently reported noncovalent inhibitors such as azaindoles and benzothiazoles will enhance the opportunities in lead optimization and lead hopping against this attractive target in Mtb. The information on ligand binding in the active site from cocrystal structures, modeling, and overlay of shape and pharmacophores can be utilized for further medicinal chemistry efforts to improve the properties of this lead series and hence progress toward a candidate drug.

EXPERIMENTAL SECTION

All anhydrous solvents, reagent grade solvents for chromatography, and starting materials were purchased from either Sigma-Aldrich Chemical Co. or Fisher Scientific. Water was distilled and purified through a Milli-Q water system (Millipore Corp., Bedford, MA). General methods of purification of compounds involved the use of silica cartridges purchased from Grace Purification systems. The reactions were monitored by TLC on precoated Merck 60 F254 silica gel plates and visualized using UV light (254 nm). All compounds were analyzed for purity by HPLC and characterized by ^{1}H NMR using Bruker 300 MHz NMR and/or Bruker 400 MHz NMR spectrometers. Chemical shifts are reported in ppm (δ) relative to the residual solvent peak in the corresponding spectra; chloroform δ 7.26,

dx.doi.org/10.1021/jm5002937 | J. Med. Chem. XXXX, XXX, XXX−XXX

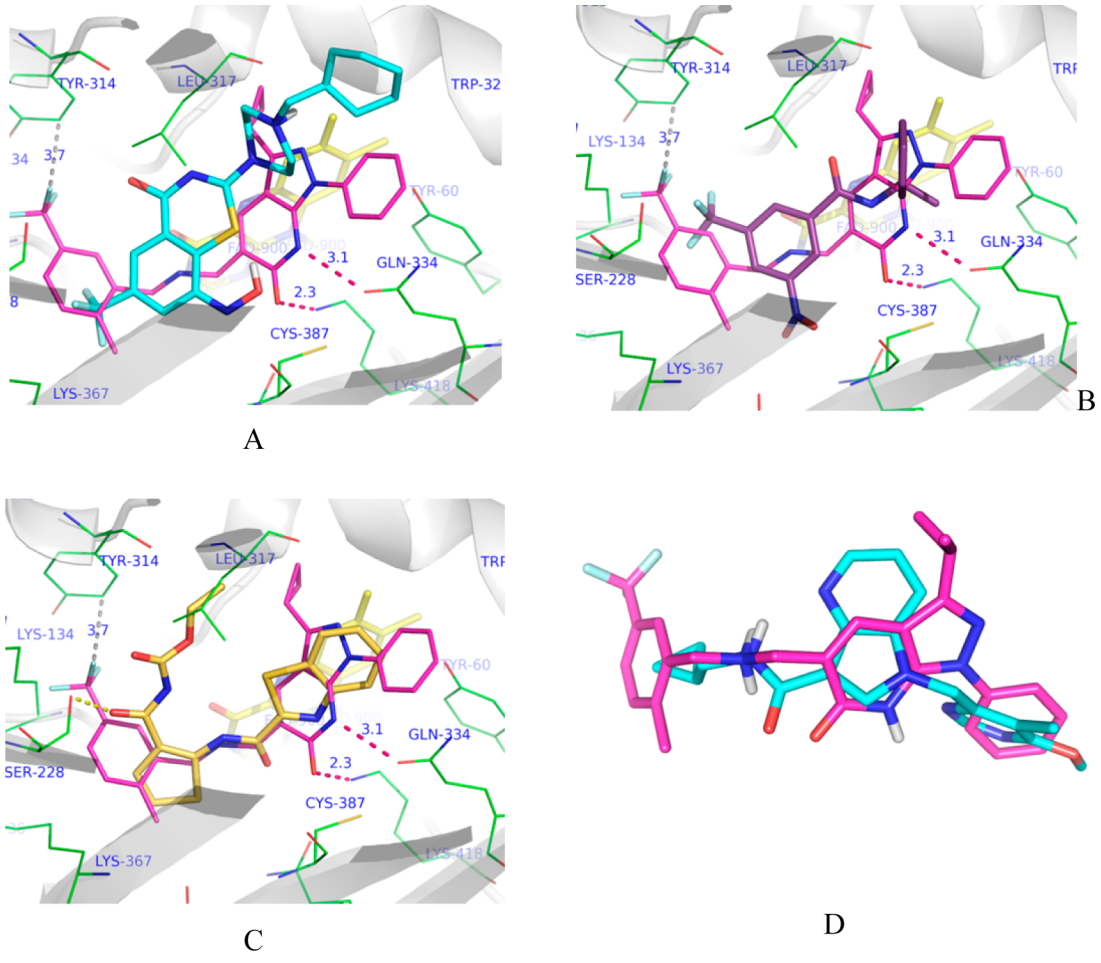

Figure 7. Overlay between the pyrazolopyridone (**19**) docking pose with crystallographic poses of **2** (A), **27** (B), **4** (C). (D) Ligand overlay between pyrazolopyridones (**19**) and azaindole (**3**).

methanol δ 3.31, DMSO-d_6 δ 3.33, and coupling constants (J) are reported in hertz (Hz) (where s = singlet, bs = broad singlet, d = doublet, dd = double doublet, bd = broad doublet, ddd = double doublet of doublet, t = triplet, tt = triple triplet, q = quartet, m = multiplet) and analyzed using ACD NMR data processing software. Mass spectra values are reported as m/z (HRMS)

All reactions were conducted under nitrogen and monitored using LCMS unless otherwise noted. Solvents were removed in vacuo on a rotary evaporator.

General Synthetic Procedures. *Reductive Amination of Pyrazolopyridone Amine with Aldehydes.* To a solution of pyrazolopyridone amine (**i**) (5.98 mmol) in methanol (30 mL) was added the corresponding aldehyde (5.98 mmol) and acetic acid (catalytic) under nitrogen. The reaction mixture was stirred for 10 min, followed by the addition of sodium cyanoborohydride (11.96 mmol). The resulting mixture was stirred at for 20 h. Then the reaction mixture was quenched by addition of aq $NaHCO_3$ and extracted with CH_2Cl_2. The combined extract was washed with water and brine and concentrated under pressure. The crude product was purified by column chromatography and subsequent PREP HPLC to provide compounds **5**–**21** with >95% purity. Compounds **22**–**26** were synthesized with minor changes in the procedure described above (see Supporting Information for details) with >95% purity.

*5-((3,4-Dimethylbenzylamino)methyl)-3-methyl-1-phenyl-1H-pyrazolo[3,4-b]pyridin-6(7H)-one (**5**).* ^{1}H NMR (300 MHz, DMSO-d_6) δ ppm 2.21 (d, J = 3.20 Hz, 6 H) 2.45 (s, 3 H) 3.73 (s, 2 H) 3.80 (s, 2 H) 7.05–7.15 (m, 3 H) 7.21 (s, 1 H) 7.47 (s, 2 H) 7.86 (s, 1 H) 8.26 (d, J = 7.91 Hz, 2 H). HRMS calculated for $C_{23}H_{24}N_4O$, 372.1950; found m/z (M + H)$^+$, 373.1940. HPLC purity: 98%.

*5-((Benzylamino)methyl)-3-methyl-1-phenyl-1H-pyrazolo[3,4-b]-pyridin-6(7H)-one (**6**).* ^{1}H NMR (400 MHz, DMSO-d_6) δ ppm 8.23 (d, J = 7.9 Hz, 2 H), 7.95 (s, 1 H), 7.48 (t, J = 7.9 Hz, 2 H), 7.41–7.32 (m, 4 H), 7.31–7.22 (m, 2 H), 3.82 (s, 1H), 3.80 (s, 2H), 2.47 (s, 3H). HRMS calculated for $C_{21}H_{20}N_4O$, 344.1637; found m/z (M + H)$^+$, 345.1711. HPLC purity: 99.1%.

*3-Methyl-5-((3-methylbenzylamino)methyl)-1-phenyl-1H-pyrazolo[3,4-b]pyridin-6(7H)-one (**7**).* ^{1}H NMR (300 MHz, DMSO-d_6): δ ppm 8.26 (d, J = 7.72 Hz, 2H), 7.87 (s, 1H), 7.46 (t, J = 7.82 Hz, 2H), 7.13–7.29 (m, 5H), 7.08 (d, J = 7.35 Hz, 1H), 3.77 (d, J = 10.36 Hz, 4H), 2.45 (s, 3H), 2.30 (s, 3H). HRMS calculated for $C_{22}H_{22}N_4O$, 358.1794; found m/z (M + H)$^+$, 359.1868. HPLC purity: 98.8%.

*3-(((3-Methyl-6-oxo-1-phenyl-6,7-dihydro-1H-pyrazolo[3,4-b]-pyridin-5-yl)methylamino)methyl)benzonitrile (**8**).* ^{1}H NMR (400 MHz, DMSO-d_6) δ ppm 8.22 (d, J = 7.6 Hz, 2 H), 8.02 (s, 1 H), 7.84 (s, 1 H), 7.76–7.69 (m, 2 H), 7.58–7.48 (m, 3 H), 7.27–7.25 (m, 1 H), 3.84 (s, 2 H), 3.76 (s, 10 H), 2.50 (s, 3H). HRMS calculated for $C_{22}H_{19}N_5O$, 369.1590; found m/z (M + H)$^+$, 370.1666. HPLC purity: 99.6%.

*5-((3-Fluorobenzylamino)methyl)-3-methyl-1-phenyl-1H-pyrazolo[3,4-b]pyridin-6(7H)-one (**9**).* ^{1}H NMR (400 MHz, DMSO-d_6) δ ppm 8.22 (d, J = 8.1 Hz, 2H), 7.97 (s, 1H), 7.48 (t, J = 7.9 Hz, 2H), 7.37 (td, J = 8.1, 6.0 Hz, 1H), 7.22 (q, J = 7.0 Hz, 3H), 7.07 (td, J = 8.6, 2.6 Hz, 1H), 3.80 (s, 2H), 3.76 (s, 2H), 2.47 (s, 3H). HRMS calculated for $C_{21}H_{19}FN_4O$, 362.1543; found m/z (M + H)$^+$, 363.1615. HPLC purity: 96.0%.

*3-Methyl-1-phenyl-5-((3-(trifluoromethyl)benzylamino)methyl)-1H-pyrazolo[3,4-b]pyridin-6(7H)-one (**10**).* ^{1}H NMR (400 MHz, DMSO-d_6) δ ppm 8.22 (d, J = 8.0, 2H), 8.01 (s, 1H), 7.76 (s, 1H),

dx.doi.org/10.1021/jm5002937 | J. Med. Chem. XXXX, XXX, XXX–XXX

7.73−7.46 (m, 5H), 7.25 (t, J = 7.4, 1H), 3.89 (s, 2H), 3.78 (s, 2H), 2.49 (s, 3H). HRMS calculated for $C_{22}H_{19}F_3N_4O$, 412.1511; found m/z $(M + H)^+$, 413.1576. HPLC purity: 96.6%.

3-Methyl-1-p-tolyl-5-((3-(trifluoromethyl)benzylamino)methyl)-1H-pyrazolo[3,4-b]pyridin-6(7H)-one (**11**). ^{1}H NMR (400 MHz, DMSO-d_6) δ ppm 8.14−8.05 (m, 2H), 7.99 (s, 1H), 7.75 (s, 1H), 7.69 (d, J = 7.4 Hz, 1H), 7.60 (dt, J = 15.1, 7.7 Hz, 2H), 7.30 (d, J = 8.2 Hz, 2H), 3.88 (s, 2H), 3.77 (s, 2H), 2.47 (s, 3H), 2.35 (s, 3H). HRMS calculated for $C_{23}H_{21}F_3N_4O$, 426.1667; found m/z $(M + H)^+$, 427.1735. HPLC purity: 99.5%.

3-Methyl-1-(pyridin-2-yl)-5-((3-(trifluoromethyl)benzylamino)methyl)-1H-pyrazolo[3,4-b]pyridin-6(7H)-one (**12**). ^{1}H NMR (400 MHz, DMSO-d_6) δ ppm 8.62−8.49 (m, 1H), 8.02 (td, J = 7.9, 2.0 Hz, 1H), 7.86 (t, J = 4.1 Hz, 2H), 7.73 (s, 1H), 7.68 (d, J = 7.1 Hz, 1H), 7.63−7.50 (m, 2H), 7.34 (dd, J = 7.3, 5.0 Hz, 1H), 3.84 (s, 2H), 3.55 (s, 2H), 2.43 (s, 3H). HRMS calculated for $C_{21}H_{18}F_3N_5O$, 413.1463; found m/z $(M + H)^+$, 414.1538. HPLC purity: 99.5%.

1,3-Dimethyl-5-((3-(trifluoromethyl)benzylamino)methyl)-1H-pyrazolo[3,4-b]pyridin-6(7H)-one (**13**). ^{1}H NMR (400 MHz, DMSO-d_6) δ ppm 7.86 (d, J = 7.3 Hz, 2H), 7.76 (d, J = 7.6 Hz, 1H), 7.71 (d, J = 7.8 Hz, 1H), 7.63 (t, J = 7.8 Hz, 1H), 4.12 (s, 2H), 3.84 (s, 2H), 3.78 (s, 3H), 2.30 (s, 3H). HRMS calculated for $C_{17}H_{17}F_3N_4O$, 350.1354; found m/z $(M + H)^+$, 351.1424. HPLC purity: 98.6%.

3-Cyclopropyl-1-phenyl-5-((3-(trifluoromethyl)benzylamino)methyl)-1H-pyrazolo[3,4-b]pyridin-6(7H)-one (**14**). ^{1}H NMR (400 MHz, DMSO-d_6) δ ppm 8.26−8.14 (m, 2H), 8.03 (s, 1H), 7.76 (s, 1H), 7.69 (d, J = 7.4 Hz, 1H), 7.66−7.53 (m, 2H), 7.53−7.42 (m, 2H), 7.30−7.20 (m, 1H), 3.89 (s, 2H), 3.78 (s, 2H), 2.27 (m, 1H), 1.19−0.89 (m, 4H). HRMS calculated for $C_{24}H_{21}F_3N_4O$, 438.1667; found m/z $(M + H)^+$, 439.1739. HPLC purity: 99.5%.

3-Cyclopropyl-1-phenyl-5-(((6-(trifluoromethyl)pyridin-2-yl)methylamino)methyl)-1H-pyrazolo[3,4-b]pyridin-6(7H)-one (**15**). ^{1}H NMR (400 MHz, DMSO-d_6) δ ppm 8.18 (d, J = 8.0 Hz, 2H), 8.06 (d, J = 7.8 Hz, 2H), 7.83 (d, J = 8.0 Hz, 1H), 7.77 (d, J = 7.7 Hz, 1H), 7.48 (t, J = 7.9 Hz, 2H), 7.24 (t, J = 7.5 Hz, 1H), 3.96 (s, 2H), 3.80 (s, 2H), 2.26 (p, J = 6.9 Hz, 1H), 1.14−0.93 (m, 4H). HRMS calculated for $C_{23}H_{20}F_3N_5O$, 439.1620; found m/z $(M + H)^+$, 440.169. HPLC purity: 98.0%.

3-Cyclopropyl-5-((2-fluoro-5-(trifluoromethyl)benzylamino)methyl)-1-phenyl-1H-pyrazolo[3,4-b]pyridin-6(7H)-one (**16**). ^{1}H NMR (400 MHz, DMSO-d_6) δ ppm 8.17 (d, J = 8.1 Hz, 2H), 8.05 (s, 1H), 7.97−7.87 (m, 1H), 7.70 (t, J = 6.7 Hz, 1H), 7.48 (t, J = 7.9 Hz, 2H), 7.41 (t, J = 9.2 Hz, 1H), 7.24 (t, J = 7.4 Hz, 1H), 3.87 (s, 2H), 3.77 (s, 2H), 2.26 (m, 1H), 1.04 (d, J = 8.4 Hz, 4H). HRMS calculated for $C_{24}H_{20}F_4N_4O$, 456.1573; m/z $(M + H)^+$, 457.1644. HPLC purity: 97.3%.

3-Cyclopropyl-5-((2-fluoro-3-(trifluoromethyl)benzylamino)methyl)-1-phenyl-1H-pyrazolo[3,4-b]pyridin-6(7H)-one (**17**). ^{1}H NMR (400 MHz, DMSO-d_6) δ ppm 8.28 (d, J = 7.8 Hz, 2H), 7.83 (s, 1H), 7.67 (dd, J = 16.1, 8.3 Hz, 2H), 7.54−7.28 (m, 3H), 7.15 (s, 1H), 3.82 (s, 2H), 3.67 (s, 2H), 2.17 (bs, 1H), 0.99 (d, J = 6.7 Hz, 4H). HRMS calculated for $C_{24}H_{20}F_4N_4O$, 456.1573; found m/z $(M + H)^+$, 457.1648. HPLC purity: 95.1%.

3-Cyclopropyl-5-(((3-methyl-6-(trifluoromethyl)pyridin-2-yl)methylamino)methyl)-1-phenyl-1H-pyrazolo[3,4-b]pyridin-6(7H)-one (**18**). ^{1}H NMR (400 MHz, DMSO-d_6) δ ppm 8.20 (d, J = 7.9 Hz, 2H), 8.02 (s, 1H), 7.86 (d, J = 7.8 Hz, 1H), 7.71 (d, J = 7.8 Hz, 1H), 7.49 (t, J = 7.8 Hz, 2H), 7.32−7.16 (m, 1H), 3.97 (s, 2H), 3.89 (s, 2H), 2.42 (s, 3H), 2.25 (m, 1H), 1.04 (d, J = 7.1 Hz, 4H). HRMS calculated for $C_{24}H_{22}F_3N_5O$, 453.1776; found m/z $(M + H)^+$, 454.1848. HPLC purity: 94.6%.

3-Cyclopropyl-5-((2-methyl-5-(trifluoromethyl)benzylamino)methyl)-1-phenyl-1H-pyrazolo[3,4-b]pyridin-6(7H)-one (**19**). ^{1}H NMR (400 MHz, DMSO-d_6) δ ppm 8.19 (d, J = 8.0 Hz, 2H), 8.05 (s, 1H), 7.80−7.65 (m, 1H), 7.50 (qd, J = 7.3, 1.9 Hz, 3H), 7.40 (d, J = 7.9 Hz, 1H), 7.24 (t, J = 7.3 Hz, 1H), 3.84 (d, J = 4.6 Hz, 4H), 2.37 (s, 3H), 2.31−2.13 (m, 1H), 1.14−0.92 (m, 4H). HRMS calculated for $C_{25}H_{23}F_3N_4O$, 452.1824; found m/z $(M + H)^+$, 453.189. HPLC purity: 99.4%.

3-Methyl-5-((2-methyl-5-(trifluoromethyl)benzylamino)methyl)-1-phenyl-1H-pyrazolo[3,4-b]pyridin-6(7H)-one (**20**). ^{1}H NMR (300 MHz, DMSO-d_6) δ ppm 8.23 (d, J = 7.91 Hz, 2H), 7.98 (s, 1H), 7.72 (s, 1H), 7.33−7.56 (m, 4H), 7.16−7.30 (m, 1H), 3.82 (s, 4H), 2.47 (s, 3H), 2.36 (s, 3H), 1.90 (s, 1H). HRMS calculated for $C_{23}H_{21}F_3N_4O$:, 426.1667; found m/z $(M + H)^+$, 427.1736. HPLC purity: 99.7%.

3-Isopropyl-5-((2-methyl-5-(trifluoromethyl)benzylamino)methyl)-1-phenyl-1H-pyrazolo[3,4-b]pyridin-6(7H)-one (**21**). ^{1}H NMR (400 MHz, DMSO-d_6) δ ppm 8.23 (d, J = 8.0 Hz, 2H), 8.12 (s, 1H), 7.74 (s, 1H), 7.51 (t, J = 7.9 Hz, 3H), 7.40 (d, J = 7.9 Hz, 1H), 7.26 (t, J = 7.3 Hz, 1H), 3.84 (d, J = 8.4 Hz, 4H), 3.38−3.22 (m, 1H), 2.37 (s, 3H), 1.40 (d, J = 6.9 Hz, 6H). HRMS calculated for $C_{25}H_{25}F_3N_4O$, 454.1980; found m/z $(M + H)^+$, 455.205. HPLC purity: 97.5%.

3-Methyl-5-((methyl(3-(trifluoromethyl)benzyl)amino)methyl)-1-phenyl-1H-pyrazolo[3,4-b]pyridin-6(7H)-one (**22**). ^{1}H NMR (400 MHz, DMSO-d_6) δ ppm 8.22 (d, J = 7.9 Hz, 2H), 8.06 (s, 1H), 7.77−7.66 (m, 2H), 7.66−7.56 (m, 2H), 7.55−7.46 (m, 2H), 7.26 (tt, J = 7.3, 1.2 Hz, 1H), 3.73 (s, 2H), 3.66 (s, 2H), 2.20 (s, 3H). HRMS calculated for $C_{23}H_{21}F_3N_4O$, 426.1667; found m/z $(M + H)^+$, 427.1744. HPLC purity: 98.3%.

3-Methyl-1-phenyl-5-((7-(trifluoromethyl)-3,4-dihydroisoquinolin-2(1H)-yl)methyl)-1H-pyrazolo[3,4-b]pyridin-6(7H)-one (**23**). ^{1}H NMR (400 MHz, DMSO-d_6) δ ppm 8.22 (bs, 2H), 8.08 (s, 1H), 7.57−7.43 (m, 4H), 7.37 (d, J = 7.9 Hz, 1H), 7.27 (dd, J = 8.1, 6.6 Hz, 1H), 3.77 (s, 4H), 2.95 (d, J = 5.9 Hz, 2H), 2.84 (t, J = 5.9 Hz, 2H), 2.51 (s, 3H). HRMS calculated for $C_{24}H_{21}F_3N_4O$, 438.1667; found m/z $(M + H)^+$, 439.1738. HPLC purity: 98.6%.

3,7-Dimethyl-1-phenyl-5-((3-(trifluoromethyl)benzylamino)methyl)-1H-pyrazolo[3,4-b]pyridin-6(7H)-one (**24**). ^{1}H NMR (400 MHz, DMSO-d_6) δ ppm 7.83 (s, 1H), 7.74 (s, 1H), 7.69 (d, J = 7.3 Hz, 1H), 7.60 (dd, J = 7.3, 5.3 Hz, 2H), 7.55 (s, 5H), 3.87 (s, 2H), 3.59 (s, 2H), 3.08 (s, 3H), 2.37 (s, 3H). HRMS calculated for $C_{23}H_{21}F_3N_4O$, 426.1667; found m/z $(M + H)^+$, 427.1735. HPLC purity: 99.1%.

1-(6-Methoxy-3-methyl-1-phenyl-1H-pyrazolo[3,4-b]pyridin-5-yl)-N-(3-(trifluoromethyl)benzyl)methanamine (**25**). ^{1}H NMR (400 MHz, DMSO-d_6) δ ppm 8.27−8.29 (m, 2 H), 8.12 (s, 1 H), 7.75 (s, 1 H), 7.68 (d, J = 7.0 Hz, 1 H), 7.61−7.48 (m, 4 H), 7.26 (t, J = 7.3 Hz, 1 H), 4.01 (s, 3 H), 3.86 (s, 2 H), 3.72 (s, 2 H), 2.50−2.51 (m, 3H). HRMS calculated for $C_{23}H_{21}F_3N_4O$, 426.1667; found m/z $(M + H)^+$, 427.1736. HPLC purity: 99.5%.

3-Methyl-6-oxo-1-phenyl-N-(3-(trifluoromethyl)benzyl)-6,7-dihydro-1H-pyrazolo[3,4-b]pyridine-5-carboxamide (**26**). ^{1}H NMR (400 MHz, DMSO-d_6) δ ppm 8.22 (d, J = 8.1 Hz, 2H), 7.97 (s, 1H), 7.48 (t, J = 7.9 Hz, 3H), 7.37 (td, J = 8.1, 6.0 Hz, 1H), 7.22 (q, J = 7.0 Hz, 3H), 7.07 (td, J = 8.6, 2.6 Hz, 1H), 3.80 (s, 3H), 3.76 (s, 2H), 2.47 (s, 3H). HRMS calculated for $C_{22}H_{17}F_3N_4O_2$, 426.1304; found m/z $(M + H)^+$, 427.1365. HPLC purity: 99.9%.

■ ASSOCIATED CONTENT

Ⓢ Supporting Information

Details of the synthesis of all compounds, biological assays, results from analogue screening, and druggability assessment from sitemap. This material is available free of charge via the Internet at http://pubs.acs.org.

■ AUTHOR INFORMATION

Corresponding Author

*Phone: +91-80-23621212. Fax: +91-80-23621214. E-mail: manoranjan.panda@astrazeneca.com.

Author Contributions

M.P., S.R., and P.S.S. are responsible for medicinal chemistry design and analyses. S.R. is responsible for synthetic chemistry. K.N. performed synthesis of some of the pyrazolopyridones. V.R. is responsible for design and analyses of microbiology experiments. V.K.S. is responsible for design and analyses of MoA and cytotoxicity studies. P.K., S.S., S.G., A.N., A.A., and N.H. performed all the microbiological and MoA experiments. V.H. and J. M. designed, performed, and analyzed the

biochemical experiments. V.P.H. designed and analyzed in vitro DMPK experiments. S.S.R is responsible for analytical chemistry experiments. A.V.R. and M.P. designed the focused library and performed the modeling and data analyses. M.P., S.R, V.R., and V.K.S wrote the manuscript.

Notes

The authors declare no competing financial interest.

■ ACKNOWLEDGMENTS

This project was funded by the Wellcome Trust under the "Affordable Healthcare in India" initiative. We acknowledge Syngene International for their contribution towards the synthesis. We are thankful to Dr. Simon Campbell for several useful discussions, suggestions during the evaluation of the project, and comments on this manuscript. We thank Dr Deborah Hawkes from the Wellcome Trust for all the support and encouragement for this project. We acknowledge Sudha Ravishankar for the *Rv3790* overexpressing strain that was used for MIC modulation studies. We thank Emma Cains and Liz Flavell from AstraZeneca, Alderley Park, for the supply of purified protein. We sincerely thank Professor G. Riccardi (University of Pavia) for providing the DprE1 expression plasmid. The support and encouragement from Dr. Prashanti Madhavapeddi, Dr. Bala Subramanian, Dr. Tanjore S. Balganesh, Dr. Bheemarao G. Ugarkar, Dr. Sunita de Sousa, Dr. Peter Warner, Dr. Ruben Tommasi, Dr. Shridhar Narayanan, and Dr. Pravin Iyer are greatly acknowledged.

■ ABBREVIATIONS USED

TB, tuberculosis; Mtb, *Mycobacterium tuberculosis*; Msm, *Mycobacterium smegmatis*; DprE1, decaprenylphosphoryl-β-D-ribofuranose-2′-epimerase; WCS, whole cell screening; MIC, minimum inhibitory concentration; MBC, minimum bactericidal concentration; BTZ, nitro-benzothiazinone; FAD, flavin adenine dinucleotide; MoA, mode of action; CFU, colony forming unit

■ REFERENCES

(1) (a) Zumla, A.; Nahid, P.; Cole, S. T. Advances in the development of new tuberculosis drugs and treatment regimens. *Nature Rev. Drug Discovery* **2013**, *12*, 388−404. (b) LeChartier, B.; Rybniker, J.; Zumla, A.; Cole, S. T. Tuberculosis drug discovery in post genomic era. *EMBO Mol. Med.* **2014**, *6*, 158−168.

(2) Barry, C. E. Lessons from seven decades of antitubercular drug discovery. *Curr. Top. Med. Chem.* **2011**, *11*, 1216−1225.

(3) Cooper, C. B. Development of *Mycobacterium tuberculosis* whole cell screening hits as potential antituberculosis agents. *J. Med. Chem.* **2013**, *56*, 7755−7760.

(4) Stanley, S. A.; Grant, S. S.; Kawate, T.; Iwase, N.; Shimizu, M.; Wivagg, C.; Silvis, M.; Kazyanskaya, E.; Aquadro, J.; Golas, A.; Dai, H.; Zhang, L.; Hung, D. T. Identification of novel inhibitors of *M. tuberculosis* growth using whole cell based high-throughput screening. *ACS Chem. Biol.* **2012**, *7*, 1377−1384.

(5) (a) Kim, J.-H.; O'Brien, K. M.; Sharma, R.; Boshoff, H. I. M.; Rehren, G.; Chakraborty, S.; Wallach, J. B.; Monteleone, M.; Wilson, D. J.; Aldrich, C. C.; Barry, C. E., III; Rhee, K. Y.; Ehrt, S.; Schnappinger, D. A genetic strategy to identify targets for the development of drugs that prevent bacterial persistence. *Proc. Natl. Acad. Sci. U. S. A.* **2013**, *110*, 19095−19100. (b) Ioerger, T. R.; O'Malley, T.; Liao, R.; Guinn, K. M.; Hickey, M. J.; Mohaideen, N.; Murphy, K. C.; Boshoff, H. I. M.; Mizrahi, V.; Rubin, E. J.; Sassetti, C. M.; Barry, C. E., III; Sherman, D. R.; Parish, T.; Sacchettini, J. C. Identification of new drug targets and resistance mechanisms in *Mycobacterium tuberculosis*. *PloS One* **2013**, *8*, e75245. (c) Farhat, M. R.; Shapiro, B.; Jesse, K.; Karen, J.; Sultana, R.; Jacobson, K. R.; Victor, T. C.; Warren, R. M.; Streicher, E. M.; Calver, A.; Sloutsky, A.; Kaur, D.; Posey, J. E.; Plikaytis, B.; Oggioni, M. R.; Gardy, J. L.; Johnston, J. C.; Rodrigues, M.; Tang, P. K. C.; Kato-Maeda, M.; Borowsky, M. L.; Muddukrishna, B.; Kreiswirth, B. N.; Kurepina, N.; Galagan, J.; Gagneux, S.; Birren, B.; Rubin, E. J.; Lander, E. S.; Sabeti, P. C.; Murray, M. Genomic analysis identifies targets of convergent positive selection in drug-resistant *Mycobacterium tuberculosis*. *Nature Genet.* **2013**, *45*, 1183−1191.

(6) (a) Riccardi, G.; Pasca, M. R.; Chiarelli, L. R.; Manina, G.; Mattevi, A.; Binda, C. The DprE1 enzyme, one of the most vulnerable targets of *Mycobacterium tuberculosis*. *Appl. Microbiol. Biotechnol.* **2013**, *97*, 8841−8848. (b) Crellin, P. K.; Brammananth, R.; Coppel, R. L. Decaprenylphosphoryl-β-D-ribose 2′-epimerase, the target of benzothiazinones and dinitrobenzamides, is an essential enzyme in *Mycobacterium smegmatis*. *PLoS One* **2011**, *6*, e16869. (c) Manina, G.; Pasca, M. R.; Buroni, S.; De Rossi, E.; Riccardi, G. Decaprenylphosphoryl-β-D-ribose 2′-epimerase from *Mycobacterium tuberculosis* is a magic drug target. *Curr. Med. Chem.* **2010**, *17*, 3099−3108.

(7) Makarov, V.; Manina, G.; Mikušovà, K.; Möllmann, U.; Ryabova, O.; Saint-Joanis, B.; Dhar, N.; Pasca, M. R.; Buroni, S.; Lucarelli, A. P.; Milano, A.; De Rossi, E.; Belanova, M.; Bobovska, A.; Dianiskova, P.; Kordulakova, J.; Sala, C.; Fullam, E.; Schneider, P.; McKinney, J. D.; Brodin, P.; Christophe, T.; Waddell, S.; Butcher, P.; Albrethsen, J.; Rosenkrands, I.; Brosch, R.; Nandi, V.; Bharath, S.; Gaonkar, S.; Shandil, R. K.; Balasubramanian, V.; Balganesh, T.; Tyagi, S.; Grosset, J.; Riccardi, G.; Cole, S. T. Benzothiazinones kill *Mycobacterium tuberculosis* by blocking arabinan synthesis. *Science* **2009**, *324*, 801−804.

(8) Makarov, V.; Lechartier, B.; Zhang, M.; Neres, J.; van der Sar, A. M.; Raadsen, S. A.; Hartkoorn, R. C.; Ryabova, O. B.; Vocat, A.; Decosterd, L. A.; Widmer, N.; Buclin, T.; Bitter, W.; Andries, K.; Pojer, F.; Dyson, P. J.; Cole, S. T. Towards a new combination therapy for tuberculosis with next generation benzothiazinones. *EMBO Mol. Med.* **2014**, *6*, 372−383.

(9) Shirude, P. S.; Shandil, R.; Sadler, C.; Naik, M.; Hosagrahara, V.; Hameed, S.; Shinde, V.; Bathula, C.; Humnabadkar, V.; Kumar, N.; Reddy, J.; Panduga, V.; Sharma, S.; Ambady, A.; Hegde, N.; Whiteaker, J.; McLaughlin, R. E.; Gardner, H.; Madhavapeddi, P.; Ramachandran, V.; Kaur, P.; Narayan, A.; Guptha, S.; Awasthy, D.; Narayan, C.; Mahadevaswamy, J.; Vishwas, K. G.; Ahuja, V.; Srivastava, A.; Prabhakar, K. R.; Bharath, S.; Kale, R.; Ramaiah, M.; Choudhury, N. R.; Sambandamurthy, V.; Solapure, S. M.; Iyer, P. S.; Narayanan, S.; Chatterji, M. Azaindoles: non-covalent DprE1 inhibitors from scaffold morphing efforts, kill *Mycobacterium tuberculosis* and are efficacious in vivo. *J. Med. Chem.* **2013**, *56*, 9701−9708.

(10) Wang, F.; Sambandan, D.; Halder, R.; Wang, J.; Batt, S. M.; Weinrick, B.; Ahmad, I.; Yang, P.; Zhang, Y.; Kim, J.; Hassani, M.; Huszar, S.; Trefzer, C.; Ma, Z.; Kaneko, T.; Mdluli, K. E.; Franzblau, S.; Chatterjee, A. K.; Johnson, K.; Mikusova, K.; Besra, G. S.; Fütterer, K.; Jacobs, W. R., Jr.; Schultz, P. G. Identification of a small molecule with activity against drug-resistant and persistent tuberculosis. *Proc. Natl. Acad. Sci. U. S. A.* **2013**, *110*, 2510−2517.

(11) Haufel, V. J.; Breitmaier, E. Synthesis of pyrazolo heteroaromatic compounds by means of 5-amino-3-methyl-1-phenylpyrazole-4-carbaldehyde. *Angew. Chem., Int. Ed. Engl.* **1974**, *13*, 604.

(12) Trefzer, C.; Rengifo-Gonzalez, M.; Hinner, M. J.; Schneider, P.; Makarov, V.; Cole, S. T.; Johnsson, K. Benzothiazinones are suicide inhibitors of mycobacterial decaprenylphosphoryl-β-D-ribofuranose 2′-oxidase DprE1. *J. Am. Chem. Soc.* **2010**, *132*, 13663−13665.

(13) Neres, J.; Pojer, F.; Molteni, E.; Chiarelli, L. R.; Dhar, N.; Boy-Röttger, S.; Buroni, S.; Fullam, E.; Degiacomi, G.; Lucarelli, A. P.; Read, R. J.; Zanoni, G.; Edmondson, D. E.; De Rossi, E.; Pasca, M. R.; McKinney, J. D.; Dyson, P. J.; Riccardi, G.; Mattevi, A.; Cole, S. T.; Binda, C. Structural basis for benzothiazinone-mediated killing of *Mycobacterium tuberculosis*. *Sci. Transl. Med.* **2012**, *4*, 150ra121.

(14) Batt, S. M.; Jabeen, T.; Bhowruth, V.; Quill, L.; Lund, P. A.; Eggeling, L.; Alderwick, L. J.; Futterer, K.; Besra, G. S. Structural basis

of inhibition of *Mycobacterium tuberculosis* DprE1 by benzothiazinone inhibitors. *Proc. Natl. Acad. Sci. U. S. A.* **2012**, *109*, 11354−11359.
(15) (a) Halgreen, T. J. Identifying and characterizing binding sites and assessing druggability. *J. Chem. Inf. Model.* **2009**, *49*, 377−389. (b) *SiteMap*, version 2.6; Schrödinger, LLC: New York, 2012.
(16) (a) *Small-Molecule Drug Discovery Suite 2013−3: Glide*, version 6.1; Schrödinger, LLC: New York, 2013. (b) Friesner, R. A.; Murphy, R. B.; Repasky, M. P.; Frye, L. L.; Greenwood, J. R.; Halgren, T. A.; Sanschagrin, P. C.; Mainz, D. T. Extra Precision Glide: docking and scoring incorporating a model of hydrophobic enclosure for protein-ligand complexes. *J. Med. Chem.* **2006**, *49*, 6177−6196.
(17) (a) Hameed, S. P.; Solapure, S.; Mukherjee, K.; Nandi, V.; Waterson, D.; Shandil, R.; Balganesh, M.; Sambandamurthy, V. K.; Raichurkar, A. K.; Deshpande, A.; Ghosh, A.; Awasthy, D.; Shanbhag, G.; Sheikh, G.; McMiken, H.; Puttur, J.; Reddy, J.; Werngren, J.; Read, J.; Kumar, M. R. M.; Chinnapattu, M.; Madhavapeddi, P.; Manjrekar, P.; Basu, R.; Gaonkar, S.; Sharma, S.; Hoffner, S.; Humnabadkar, V.; Subbulakshmi, V.; Panduga, V. Optimization of pyrrolamides as Mycobacterial GyrB ATPase inhibitors: structure−activity relationship and in vivo efficacy in a mouse model of tuberculosis. *Antimicrob. Agents Chemother.* **2014**, *58*, 61−70. (b) Kale, M. G.; Raichurkar, A. K.; Shahul, H. P.; Waterson, D.; McKinney, D.; Manjunatha, M. R.; Kranthi, U.; Koushik, K.; Jena, L.; Shinde, V.; Rudrapatna, S.; Barde, S.; Humnabadkar, V.; Madhavapeddi, P.; Basavarajappa, H.; Ghosh, A.; Ramya, V. K.; Guptha, S.; Sharma, S.; Vachaspati, P.; Kumar, K. N.; Giridhar, J.; Reddy, J.; Panduga, V.; Ganguly, S.; Ahuja, V.; Gaonkar, S.; Kumar, C. N.; Ogg, D.; Tucker, J. A.; Boriack-Sjodin, P. A.; de Sousa, S. M.; Sambandamurthy, V. K.; Ghorpade, S. R. Thiazolopyridine ureas as novel antitubercular agents acting through inhibition of DNA Gyrase B. *J. Med. Chem.* **2013**, *56*, 8834−8848. (c) Shirude, P. S.; Madhavapeddi, P.; Tucker, J. A.; Murugan, K.; Patil, V.; Basavarajappa, H.; Raichurkar, A. V.; Humnabadkar, V.; Hussein, S.; Sharma, S.; Ramya, V. K.; Narayan, C. B.; Balganesh, T. S.; Sambandamurthy, V. K. Aminopyrazinamides: novel and specific GyrB inhibitors that kill replicating and nonreplicating *Mycobacterium tuberculosis*. *ACS Chem. Biol.* **2013**, *8*, 519−523.
(18) *ROCS 3.2.0.4*; OpenEye Scientific Software: Santa Fe, NM, 2013; http://www.eyesopen.com. (b) Hawkins, P. C. D.; Skillman, A. G.; Nicholls, A. Comparison of shape-matching and docking as virtual screening tools. *J. Med. Chem.* **2007**, *50*, 74−82.